Journal of Materials Processing Technology, 31 (1992) 413-440
Elsevier

Rupert's glass drops: Residual-stress measurements and calculations and hypotheses for explaining disintegrating fracture

W. Johnson[1]

Schools of Engineering, Potter Research Centre, Purdue University, West Lafayette, IN 47907, USA

S. Chandrasekar

School of Industrial Engineering, Purdue University, West Lafayette, IN 47907, USA

(Received June 20, 1991; accepted August 23, 1991)

Industrial Summary

Tear-shaped drops of glass known as Prince Rupert's drops, formed by quenching molten glass, have been an object of scientific curiosity ever since they were introduced into the English King Charles II's court in the mid-seventeenth century. These drops exhibit some unusual characteristics, the most prominent of these being that they shatter into powder when moderate finger pressure, sufficient to initiate a local fracture, is applied to the tail of the tear-drop.

Density, temperature and residual-stress measurements have been made on Rupert's drops made of three glasses - flint, Pyrex and 80% silica; the temperature measurements have also been used to calculate the residual-stress distribution in these drops. These elements of information have been used to provide an explanation for the "unusual" disintegration of these drops when damaged; the explanation involves stress-wave generation and propagation with associated fracturing.

1. Introduction

What became known as Prince Rupert's drops was introduced to the Royal Society of London in 1660–61 at the request of King Charles II. He asked for an explanation of the nature of the drops, having received them in the first place from his nephew Prince Rupert. The earliest major study of these drops was published by Robert Hooke [1] and Fig. 1 in particular is the best known illustration of them. They are simply drops of solidified glass; they are formed by allowing molten glass from the end of a heated rod to fall from a modest height into water, which moderates the speed at impact and finally fully cools the drop. Separation of the drop from the rod – a viscous process – is respon-

[1]Also Emeritus Professor, Engineering Department, University of Cambridge, UK.

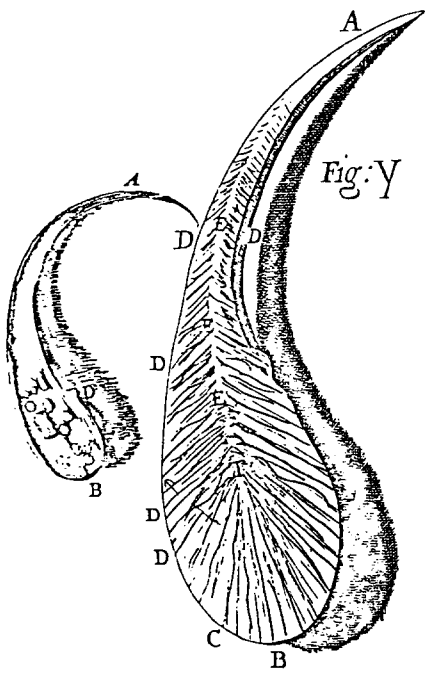

Fig. 1. "Prince Rupert's Drops" as they appear in Hooke's *Micrographia*: an intact drop with bubbles and a fractured drop when preserved by the application of a coating of fish glue.

sible for the long-drawn out tail. The general features of the formation and cooling phenomena involved were well understood and originally described by Hooke [1]. It will suffice here to refer to the recent lengthy paper by Brodsley et al. [2], wherein there is a discussion of the literary, historical and scientific features of this subject.

The glass drops of Rupert in themselves are a play-thing, a scientific curiosity only valuable for affording a study of such matters as the transient cooling of a drop with a phase change, and the consequent development of a system of residual stresses. The latter – an internally equilibrated stress system – is important for understanding the disintegration of a drop when a portion of it is damaged, the internal stresses unsuccessfully attempting to re-adjust themselves to the new geometry.

What the authors have attempted to do below is to make measurements of density, temperature and residual-stress distribution, taking advantage of present-day techniques; these then provide, among other things, a basis for better elucidating the fracturing process when, say, the tip of a drop is broken. The authors have also used one of the former elements of information – the temperature measurements – as a basis for calculations of the stress distribution in a drop.

The forming of lead shot drops is similar in many respects to the formation of Prince Rupert's drops. The discovery of lead shot drop-forming is again attributed to Prince Rupert, but likely was seen by him in Europe before returning to Charles II's England in the 1660s. This process, however, was not always a toy but later became the basis of a small industry having military and hunting associations. The process was industrially successful after about 1790 and for about 150 years thereafter, for the production of solid spherical shot i.e., when tails were not present. For this, the addition of a small amount of a chemical substance (arsenic trisulphide or auripigmentum) to the original lead pigment was imperative; this caused a faster contraction and adaptation from a tear drop shape to a sphere. It also required short towers to be introduced – an innovation made by William Watts of Bristol in 1782. A short history and the scientific facets of this process were reviewed by Johnson et al. [3], but have recently been more comprehensively laid out in Johnson [4]. However, as implied above, this industrial process has, over the last thirty or forty years, become obsolete. In this process the larger the size of the shot required, the greater was the required height of fall down the drop towers. Shot towers can still be seen, where communities with a regard for preserving historical industrial artifacts are to be found. Ancient drop towers, like castles, can be regarded as industrial archaeology that merit attention and reclamation.

2. Experiments

Tear-shaped drops of flint, borosilicate (Pyrex) glass and 80% silica glass (henceforth referred to as silica) were prepared for experimental study. Table 1 gives the nominal thermophysical properties of these glasses [5]. The drops were made by melting glass rods using a welding torch which was clamped at a fixed distance of 0.5 inch (1 inch = 25.4 mm) from the glass rod tip, so as to obtain repeatable heating conditions. The molten drops were allowed to fall freely in air through distances ranging from 3 to 42 inches into a beaker of

TABLE 1

Thermo-physical properties of the three glasses

Type of glass	Coefficient of thermal expansion ($\times 10^7$) (cm/cm°C)	Melting temperature (°C)	Thermal[a] shock resistance (°C)
flint	93.5	-	50 to 70
Pyrex (borosilicate)	40 to 50	≈1300 to 1400	120 to 160
silica	5 to 10	≈1800	>300

[a]Based on plunging the sample into cold water after oven heating. A resistance of 100°C implies no breakage if heated to 110°C and plunged into water at 10°C.

water. The depth of water in the beaker was kept, in general, at around 12 inches. The bottom of the beaker was covered with a layer of sand, on top of which a filter paper was placed to receive the drops. It was generally observed that in the absence of a sand–filter paper combination at the bottom of the beaker, flint glass-drops shattered on impact with its bottom surface. The purpose of the sand–filter paper combination was to cushion the drops against the effects of impact. Shattering was only occasionally observed with Pyrex glass-drops and never with the silica glass.

Figure 2(a) shows a photomicrograph of a typical Rupert drop as produced by the present method, whilst Fig. 2(b) is a photomicrograph of the fractured head of the drop preserved by the application of a coating of epoxy. The head of a drop is roughly hemispherical of about 5 mm in diameter, while the tail portion is approximately conical and extends to a distance of about 8 mm. By carefully controlling the flame temperature, the rate of heating of the glass rod, and the distance between the rod and the water surface in the beaker, the tail of a drop could easily be made extremely long and slender (less than 1 mm in diameter). It was found possible to produce drops with tails as long as 43 inches; Brodsley et al. [2] have also made similar observations. Sometimes, drops remained suspended in water, having failed to separate from the parent rod at the tail.

3. General observations on the nature of the glass drops

Close examination of the glass drops prepared in the present experiments revealed several qualitative features.

(i) Pyrex and silica glass drops do not exhibit the "typical fracture" characteristics observed with flint glass. If a modest finger pressure sufficient to cause local fracture is applied to the tail of a Pyrex or silica drop, it does not cause it to shatter into powder as does flint but, rather, a small piece of the tail breaks off leaving the rest of the drop intact. With flint glass, under similar circumstances, a multitude of cracks propagate with a "popping" noise, leaving behind a powdery dust of glass particles. A point to be noted here is that the leading or head portion of a drop usually remains intact even though the glass within it has shattered into a powder, see Fig. 2(b). Gentle pressure applied to the head, after popping, results in its disintegration. The head portion is usually well preserved with the powdery particles intact, if it is coated with a thick layer of epoxy before pressure is applied at the tail. Similar differences in the fracture behaviour of flint, Pyrex and fused silica are also observed during thermal shock resistance tests conducted on these materials [5]. A typical thermal shock resistance test conducted in the glass industry consists of plunging a standard glass sample into cold water after oven heating [5]. Based on such a test, thermal shock resistance numbers such as those in Table 1 are determined. A thermal shock resistance of 100°C (212°F) does not cause

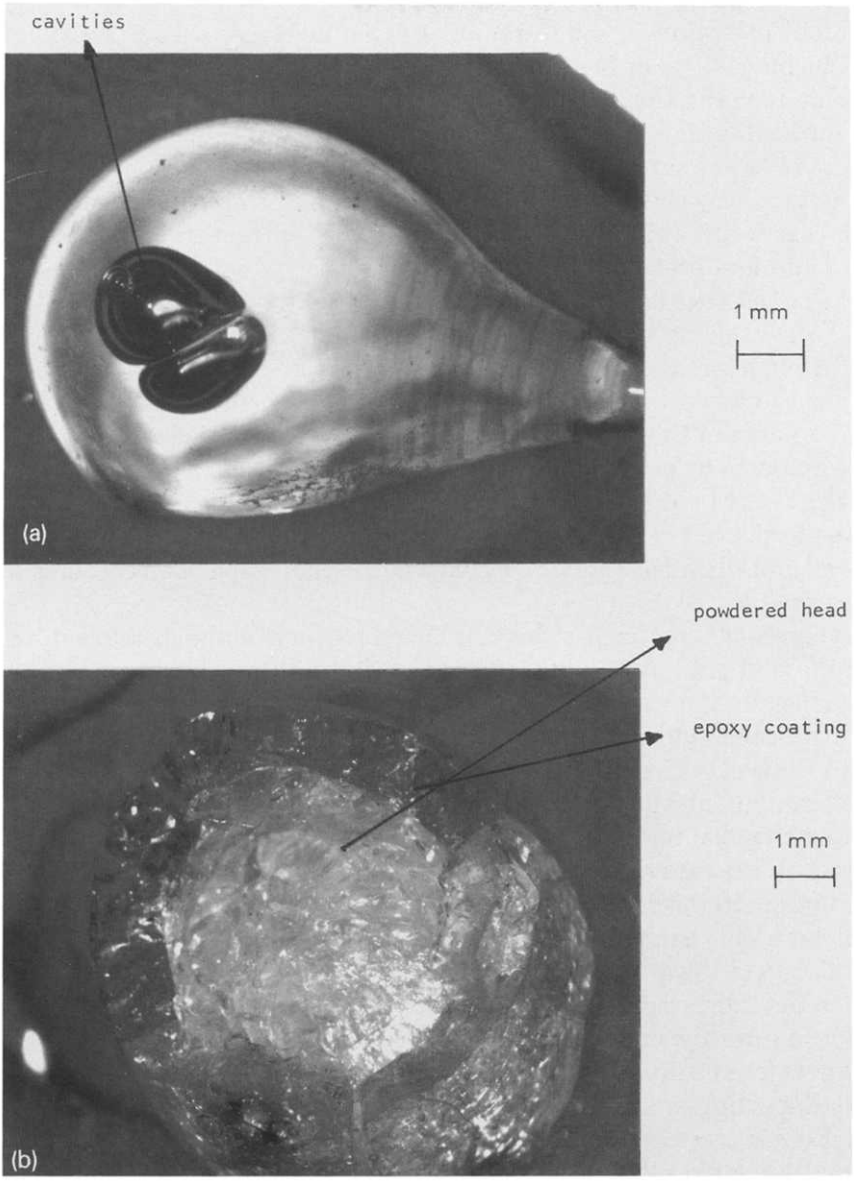

Fig. 2. Photo-micrograph of: (a) typical "Rupert's Drop" (note the cavities); and (b) the fractured head of the drop preserved by the application of a coating of epoxy.

breakage of the standard sample if heated to 110°C (230°F) and plunged into water at 10°C (50°F). It may be seen from Table 1 too, that silica glass has the highest shock resistance and flint the lowest. The fracture of glass drops made of different materials, in the present study, also follows a similar trend.

It is pointed out in Bansal and Doremus [6] that materials with a lower thermal expansion coefficient have a higher thermal shock resistance. The interrelationship between these properties and the transient thermal stresses developed during the cooling of glass is thought to be significant [6].

(ii) The close examination of flint drops shows the presence of bubbles or cavities (which may or may not contain gases), some of which are near to the drop axis centre-line and some close to the surface. Typically, these drops have between 2 and 4 cavities but as many as six were observed sometimes. In Pyrex, the number of cavities is usually smaller than in flint – typically only 1 or 2 are produced when using a propane torch, the flame temperature of which is 1350°C. When a torch with a flame temperature greater than 1350°C (such as oxyacetylene) was used, the Pyrex drops produced by melting and quenching showed a number of tiny bubbles, typically 3 or more. The silica drops, which had to be prepared by heating to temperatures of between 1750°C and 1800°C, rarely had any bubbles. Thus, thermal expansion appears to play an important role in the formation of these cavities. It may be observed from Table 1 that both Pyrex and silica have significantly lower thermal expansion coefficients than flint glass.

(iii) A series of experiments was conducted by varying the distance of fall between the flint glass-rod and the water surface (in the beaker) to between 4 and 42 inches in steps of 4 inches. The filter paper–sand combination was removed from the bottom of the beaker, but the water depth was kept at 12 inches. In these cases, it was found that glass drops which fell through a distance greater than about 30 inches consistently shattered on contact with the bottom of the beaker but drops that travelled less than 4 inches in air did not. An analysis of the experimental results revealed that about 50% of the drops shattered when dropped from a height of 30 inches, compared with only 14% for 10 inches. This experiment demonstrated clearly that it was the higher impact velocity of the drops in combination with the quenching rate that contributed to their disintegration.

(iv) The nature and curling of the tail of a drop appears to be related to the manner in which the drop impinges upon and enters the water surface.

(v) On annealing, the flint glass drops lost their initial fracturing characteristics. Finger pressure applied to the tail of these drops no longer caused shattering. Similar results were obtained with flint glass-drops prepared by quenching in air and in carbon tetrachloride. It should be pointed out that glass drops prepared by quenching in air remained in a pliable viscous state even after falling through heights of up to 6 feet. Annealing of the flint and Pyrex glass-drops also resulted in the disappearance of the internal bubbles.

(vi) When molten flint glass-drops were quenched by dropping them into a flask of liquid nitrogen at 77°K, nearly immediate disintegration occurred on entering the liquid nitrogen, in a number of instances. This is in dramatic contrast to the flint glass-drops quenched in air.

(vii) A flint glass drop, of about 5 mm in diameter at its head, was placed in a solution of hydrofluoric acid (about 30% by volume concentration) until about 0.5 mm of the skin was etched away. The drop was then removed and cleaned carefully in water. When finger pressure was applied to the tail of the drop the whole of it broke into pieces; but the pieces into which it fractured were much larger than when broken in the usual manner. The experiment was repeated with more flint drops mostly resulting in similar results. Thomson (1889) [7][2] made similar observations in his early studies.

These qualitative observations, especially the annealing results, the disintegration of the flint glass drops on contact with the bottom face of the beaker, and the material dependence of the fracture characteristics of the glass drops, reinforce the idea that residual stresses play an important role in the unique fracture phenomenon observed with "Rupert's drops".

Attention is now turned to quantitative characterizations concerning these glass drops.

4. Density measurements

The densities of the glass drops were determined by weighing them using a digital balance in air and in water. All the drops were prepared by quenching in water and by keeping the distance of fall in air at 42 inches. Table 2 gives the mean densities of the different glass drops before and after annealing. It appears that there is a small increase in the density of the flint glass after annealing. In contrast, the density changes in the Pyrex and silica drops after annealing are insignificant. Of course, these latter drops contained few or no observable bubbles in contrast to the flint drops. Thomson [7] also observed a similar small increase in the density of flint glass drops.

TABLE 2

Mean densities of glass drops formed by quenching

Type of glass		Density[a] (g/cm^3)
flint:	before annealing	2.533
	after annealing	2.563
Pyrex:	before annealing	2.287
	after annealing	2.291
silica:	before annealing	2.183
	after annealing	2.188

[a]The densities were obtained as an average of measurements on 12 drops: error ± 0.003 g/cm^3.

[2]In Brodsley et al. [2], this is mistakenly taken to be Lord Kelvin.

5. Temperature measurements on Rupert's drops

The temperature of a drop was measured at various heights during its fall. The purpose of these measurements was to:

(1) determine the initial temperature of the drop as it leaves the glass rod and also to obtain its temperature when it enters the water; this then enables an estimate of the degree of its cooling in air to be made;

(2) obtain the approximate drop temperature at various times after it has entered the water; this then enables the temperature boundary conditions to be established for residual-stress calculations;

(3) provide experimental results which serve to check the analytical cooling models for drops falling through air.

The temperature measurements were carried out by using a multiple element infra-red sensor. Figure 3 shows a schematic of the temperature measurement set-up. The multiple element sensor used in the present experimental study consisted of 4 individual indium antimonide cells mounted on a Dewar and cooled with liquid nitrogen. This serves to minimize the "noise" and improve the temperature measurement sensitivity. Each of the 4 sensor elements had a time constant of 6.8 μs and a spot size of 40 μm at the working distance used in the present study, i.e., the sensor estimated the temperature over a spot of this diameter. With the present 4-element sensor, the temperature measurements could be made simultaneously at 4 locations. The radiation mea-

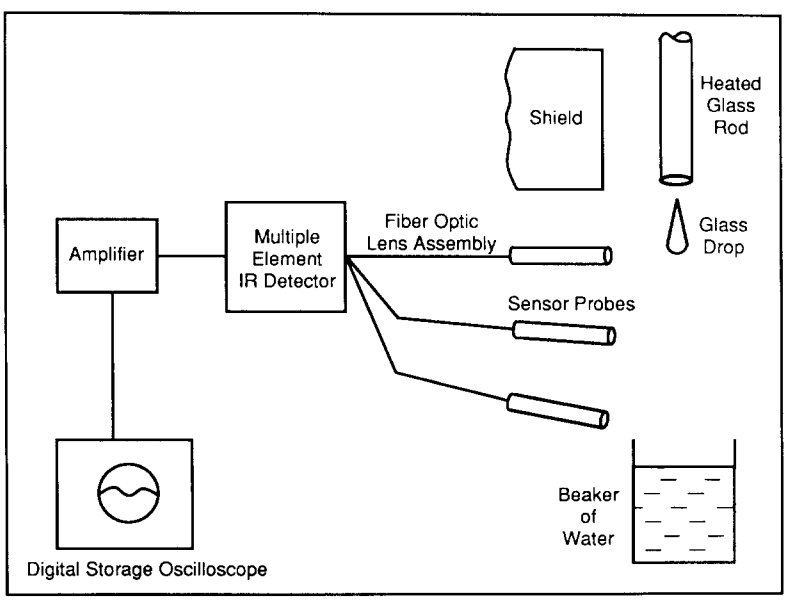

Fig. 3. Schematic of the set-up to measure the temperature of a "Rupert's Drop" at various stages during solidification.

surements were made in the spectral range 4.8 to 5.6 μm, where the emissivities of all the three glasses are high and also the absorption bands of atmospheric water vapour and carbon-dioxide are mostly negligible. Dual-wavelength radiation measurements were carried out in this wavelength window using optical radiation filters to obtain the temperature of the glass-drop. Details of this measurement procedure are given in Chandrasekar et al. [8]. The temperature measuring range of accuracy of the sensor under these conditions was $\pm 7.5°C$.

Fiber-optic lens assembly probes were used to pick up the radiation from four different positions in the path of the drop and to focus it at the detector plane, the output of each detector element being recorded in a digital storage oscilloscope. Emissivity corrections were made electronically in the sensor circuit, based on dual measurements. A calibration test was also carried out to check the cross-sensitivity between the detector elements, such as the change in the output of an element due to radiation from the glass drop being incident on adjacent elements, the technique of Hartley et al. [9] being used for this purpose. The maximum "cross-talk" was about 2% from adjacent elements in the present study, the results reported not being adjusted for it.

Three different glass rods, viz., flint, Pyrex and 80% silica, were investigated in the forming of the glass drops. Figure 4(a) shows a typical oscilloscope trace of the temperature signal from the drop surface, just as the drop passes across one of the measuring probes, whilst Fig. 4(b) shows its surface temperature history at various stages of its fall in air. The point at which the curves terminate in the figure gives the temperature of the drop just before entering the water. From this figure, it can be seen that the temperature change in air is approximately the same for all three glasses, being in the range 70° to 110°C.

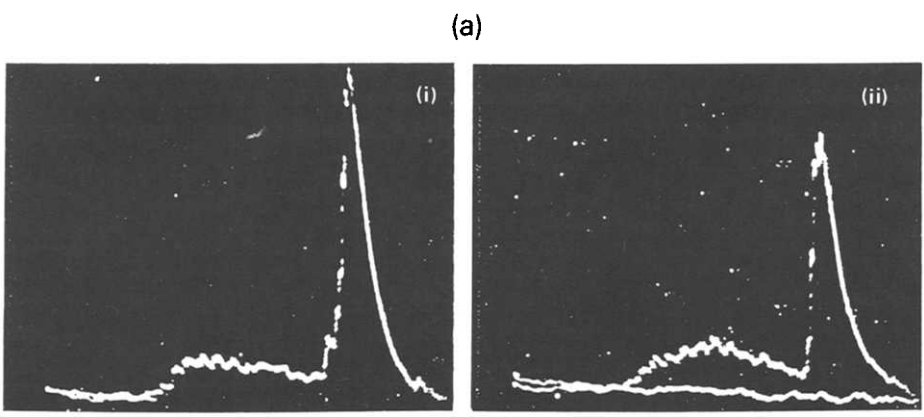

Fig. 4. Temperature measurement results: (a) oscilloscope traces of the infra-red temperature signal from a flint glass drop at two points during solidification: (i) just as it leaves the glass rod (peak temperature ca. 1180°C); (ii) before touching the water surface (peak temperature ca. 1110°C).

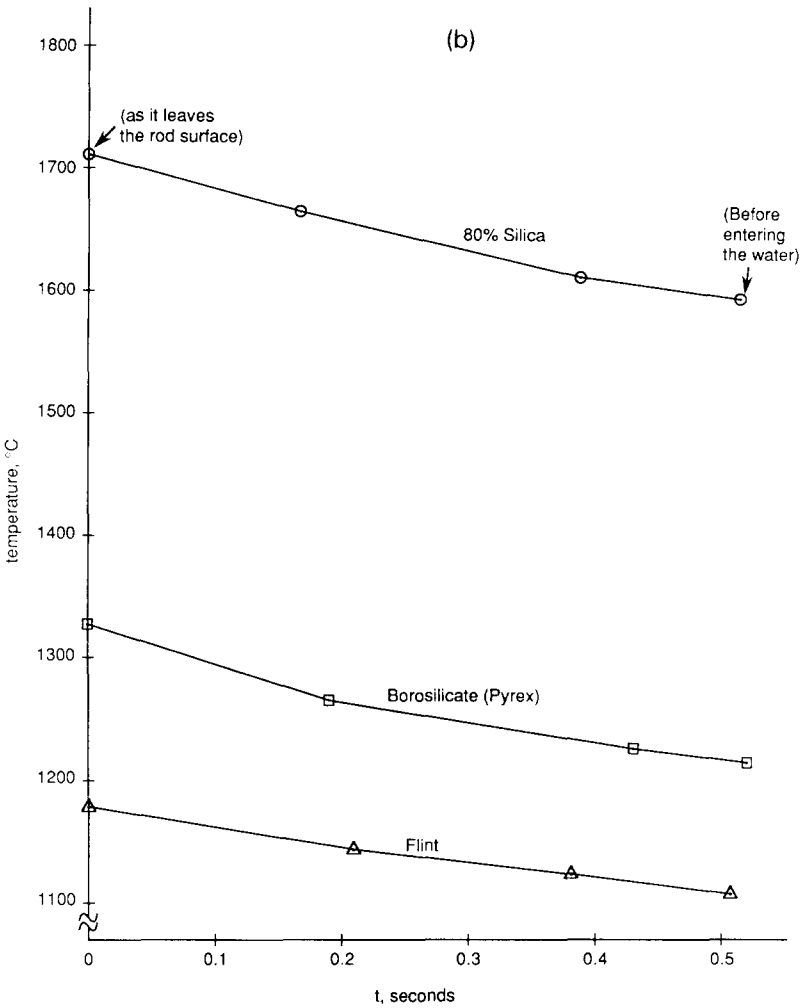

Fig. 4 (continued) (b). The measured surface temperature of three different glass drops during solidification in air.

Silica drops experienced the greatest temperature decrease of ca. 110°C and flint drops the least at ca. 70°C. Surface temperature as measured here is actually an average temperature over a small volume near the surface. The measurements also show that the glass drop, as it hits the water surface, is essentially molten. The temperature at this point is taken to be the initial surface temperature for the present residual-stress analysis calculations.

The cooling of the glass drop in air was modelled analytically, the drop shape being approximated to that of a sphere of a certain diameter. The analysis involved in solving the heat conduction equation with mixed radiation and convection boundary conditions at the surface of the drop and such problems

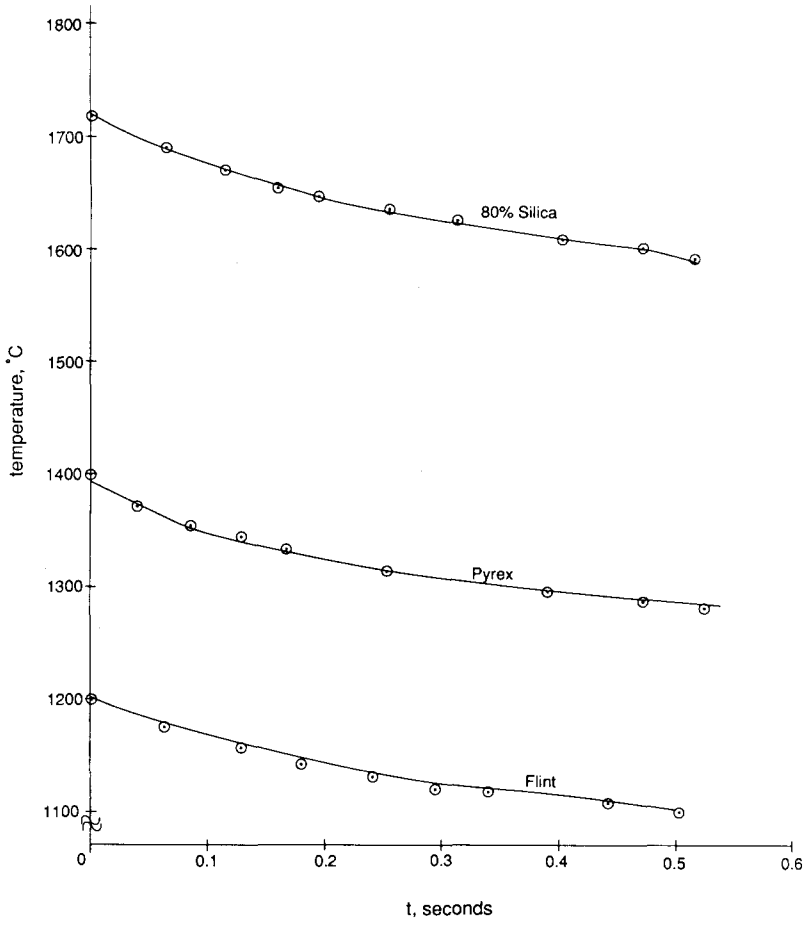

Fig. 5. Analytically calculated surface temperature of three different glass drops during solidification in air.

are discussed in Carslaw and Jaeger [10], Jaeger [11] and Mann and Wolf [12]. A numerical finite difference scheme was used.

Figure 5 shows the temperature–time history at a point on the surface of the glass spheres, obtained from the numerical analysis. The temperature decrease in air was about 93°C for flint and about 122°C for silica, which are close to presently measured values.

From this combination of analytical and experimental investigation of the temperature it is reasonable to assume the measured surface temperature of a glass drop as it enters the water surface to be the starting temperature for the total solidification process in water. Details of the residual-stress calculation are described in a later section.

The function of the water, as remarked above, is generally assumed to be

that of "catching" the drop and reducing its impact speed. Present measurements show that the temperature of the drops is between 1000°C and 1600°C when they enter the surface of the water. At these temperatures all the drops are in a "nearly" molten state and water, therefore, provides an additional function as a quench medium for solidification.

The water ambient temperature was 25°C. In order to estimate the time taken by the drop to cool down to this temperature (which is necessary to know for the residual-stress calculations), it is essential to make temperature measurements on the glass drop in the water. However, the scattering of infra-red radiation by the water makes this very difficult. An approximate estimate of the time taken for the glass drop to cool to 25°C was obtained as follows. By manipulating the drop generation process, one could create Rupert's drops with a long tail such that the drop remained attached to the glass rod even after entering the water. It was then pulled out at periodic intervals and into the focal plane of the detector, the surface temperature now being measured with the infra-red sensor. A thin film of water remains attached to the glass drop which causes scattering of the IR radiation emitted by it. Therefore only an approximate estimate of the surface temperature of the glass drop is obtained. By a series of measurements on a single drop, it was found that the ambient temperature was attained after a period of about 145 seconds. This thus enabled a suitable cooling process model to be developed for determining the residual-stress distribution.

6. Residual-stress measurements

The qualitative observations made on Rupert's drops (in Section 3) indicate that residual stresses, if any, are developed during the solidification of a glass drop in water and may play an important role in their fracture. It was therefore decided to attempt to measure the residual stresses in particular along the centre-line and near to the surface, induced in these drops during solidification. Even in materials such as glass, which macroscopically behave elastically at room temperature, residual stresses are induced by such processes as tempering and grinding (Gardon [13]; Johnson-Walls et al. [14]). The origin of residual stresses in tempering lies in the viscoelastic behaviour and the structural changes occurring across the glass transition temperature. In contrast, grinding residual stresses are probably due to a limited amount of plastic deformation taking place within the glass during its indentation by the abrasive. That glass can deform plastically is seen in the experiments of Bridgman [15], who showed that glass specimens undergo a limited amount of permanent deformation in tension tests carried out under hydrostatic pressure. More recently, Hagan and co-workers [16,17] have demonstrated the presence of shear flow lines underneath Vickers indentations in soda-lime glass.

A survey of residual-stress measurement techniques indicated that the cur-

vature technique (Treuting and Reed [18]) is most suitable for assessing the residual stresses in the present work. X-ray diffraction is not suitable for estimating residual stresses in glass in view of its amorphous nature while the use of the photoelastic technique is limited by the solidity and complex geometry of the drop.

The Appendix gives details of the curvature technique that was used and which has been used extensively by a number of other investigators to measure the residual stresses on the surfaces of ceramics and metals.

The average residual-stress distributions in a Rupert drop near to the centreline and near to the surface were investigated. Glass drops of diameter at least 10 mm (of the hemisphere) and length at least 22 mm were prepared. They were coated with a thick layer of water-soluble epoxy and then rectangular specimens of glass were cut out of the drop from along its axis and from near to its surface using a diamond wafering blade: the location of these specimen areas is shown in Fig. 6. Considerable effort and extreme care was needed to make these specimens, because many of them repeatedly fractured or crumbled during the cutting process. A very small down-feed rate for the diamond blade (fixed by trial-and-error), a highly stiff machine spindle and a minimum of machine tool vibration (achieved by the use of a computer numerically controlled machine) were necessary to avoid this breakage.

The cut specimens were mounted in epoxy in a holder and the initial curvature of the reference surface (see the Appendix) was traced with a profilometer. The specimens were then polished with a 1 μm diamond paste followed by a 0.5 μm magnesium oxide polishing slurry. The sample preparation pro-

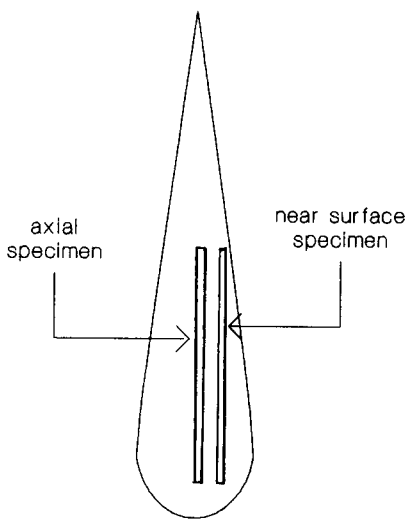

Fig. 6. Locations from which specimens were cut out from the glass drops for residual-stress measurements.

cedure was in many respects similar to the preliminary techniques used to form thin specimens for transmission electron microscopy. The nominal sizes at the end of this polishing step were for specimens cut from near to the axis, ca. 7 mm long × 2 mm wide × 1.5–2.0 mm thick and for specimens cut from near the surface, ca. 5 mm long × 2 mm wide × 1.5–2.0 mm thick.

The side faces of the specimen were coated with epoxy whilst the two parallel faces – the 7×2 mm in one specimen and the 5×2 mm in the other – were left

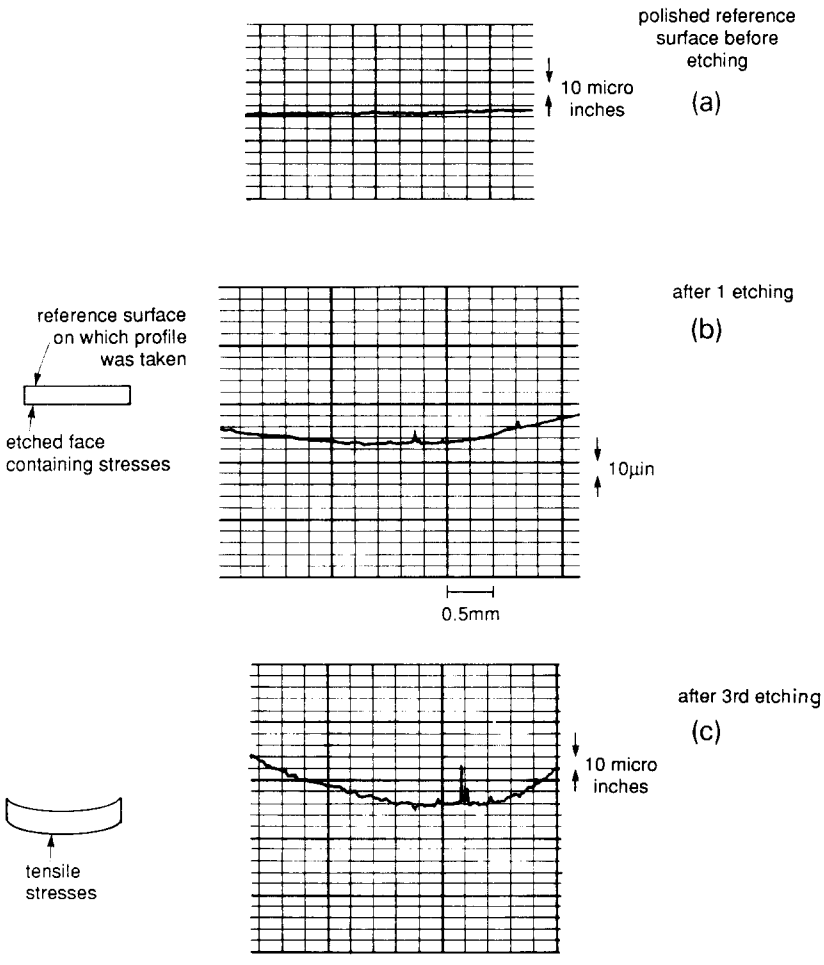

Note The nature of curling of the reference surface indicates tension on the etched surface.

Fig. 7. Talysurf profilometer traces across the length of the "reference" surface (Appendix) of a specimen cut out from near the drop-axis centre-line (see Fig. 6) of a flint glass drop: (a) polished "reference" surface before etching; (b) "reference" surface after one etching; and (c) after the third etching.

TABLE 3

Elastic constants of the three different glasses

Type of glass	Poisson's ratio	Young's modulus ($\times 10^{-6}$) (lb/in^2)[a]
flint	0.22	10
Pyrex	0.22	10
silica	0.20	10

[a] $1\ lb/in^2 = 6.89\ kN/m^2$

uncoated. One face of each of these specimens was etched with a 7% (concentration by volume) solution of hydrofluoric acid. The reference surface, see the Appendix, was traced with a profilometer in two perpendicular directions after each etching step. Each specimen was etched three times, the amount of material removed being determined as in the Appendix. Figure 7 shows some typical profilometer traces obtained from a flint glass specimen cut from near the axis of the drop. The direction, or nature of the curl of the specimen, indicates that tensile residual-stresses exist in the specimen in the axial direction. From measurements of the curvatures, of the amount of material etched away and of the elastic constants of the various glasses (see Table 3), the residual stresses in the specimen were determined using the equations of the Appendix.

Figures 8(a) and 8(b) show the residual stresses measured in flint glass and silica using this curvature method. The measurements were carried out on five specimens for each of these two materials, the results for both being reproduced in Figs. 8(a) and 8(b). The measured average residual stresses in both of the flint glass specimens are tensile near to the axis, see Fig. 8(a), and are of a fairly high magnitude, approximately 1700 to 4400 lb/in^2 ($1\ lb/in^2 = 6.89\ kN/m^2$) in the axial direction and about 3600 to 6200 lb/in^2 in a direction perpendicular to the axis. However, in the case of the silica specimens, the corresponding tensile stresses near to the axis are significantly lower at ca. 0–700 lb/in^2 in the axial direction and ca. 200–800 lb/in^2 in a direction perpendicular to the axis (see Fig. 8(a)).

The residual stresses near the surface of the drop as seen from Fig. 8(b) are compressive in both silica and flint. Again, the magnitude of these stresses is higher in flint glass at ca. 3400–14000 lb/in^2 than it is at 400–2200 lb/in^2 in silica.

For reference purposes, residual stresses were also measured on specimens cut out of a flint glass-drop that was annealed. This was done by heating the glass to 800 °C followed by slow cooling, all within a furnace, the furnace temperature of which was brought down to room temperature in steps of 50 °C, every half hour. Figure 8(c) shows the measured residual stresses in these

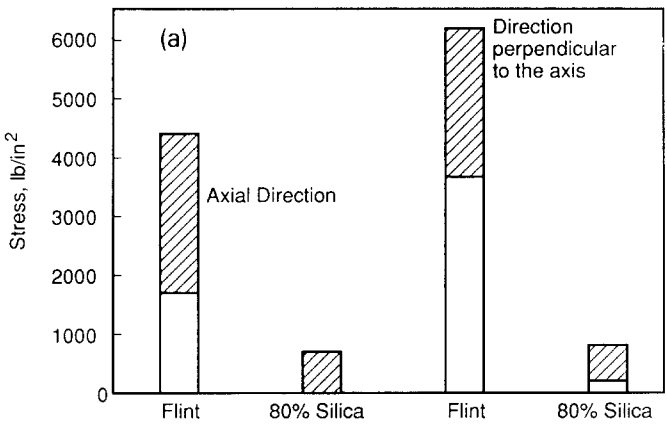
(a)
Direction perpendicular to the axis
Axial Direction
Stress, lb/in2
6000
5000
4000
3000
2000
1000
0
Flint
80% Silica
Flint
80% Silica

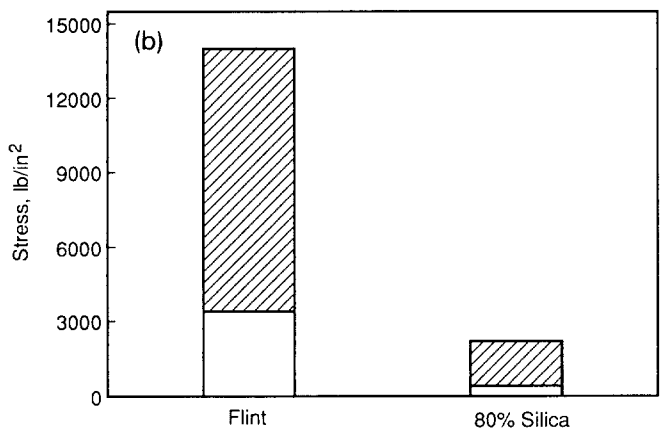
(b)
Stress, lb/in2
15000
12000
9000
6000
3000
0
Flint
80% Silica

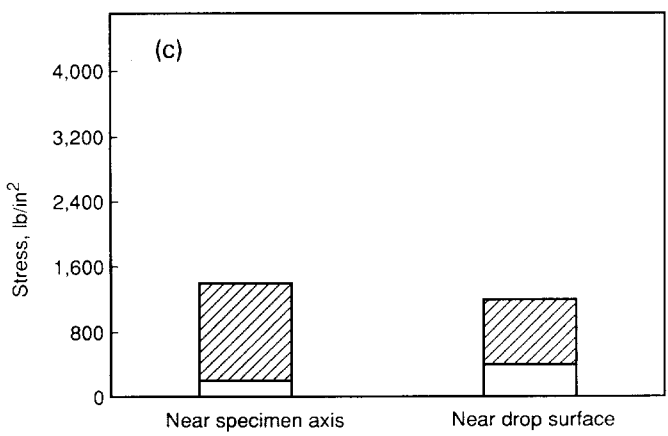
(c)
Stress, lb/in2
4,000
3,200
2,400
1,600
800
0
Near specimen axis
Near drop surface

specimens; they are compressive at ca. 200–1400 lb/in^2, both near to the axis and close to the surface.

Two questions that naturally arise in the context of these residual-stress measurements are: (i) are the measured residual stresses those induced by solidification of the glass drop or (ii) are they those induced by the diamond slicing and polishing process? To answer these questions the following further investigation was conducted.

Residual-stress measurements were carried out on flat rectangular flint glass specimens ca. 50 mm × 25 mm × 2 mm thick that had been generated by slicing with a diamond wheel and magnesium oxide polishing only or proceeding in a manner similar to that used to generate the residual-stress specimens from a Rupert drop. Figure 9 shows these results. The residual stresses induced by the slicing process are dominantly biaxially compressive near to the surface at around 2000 lb/in^2 and become tensile below a depth of about 0.0007 inch; see

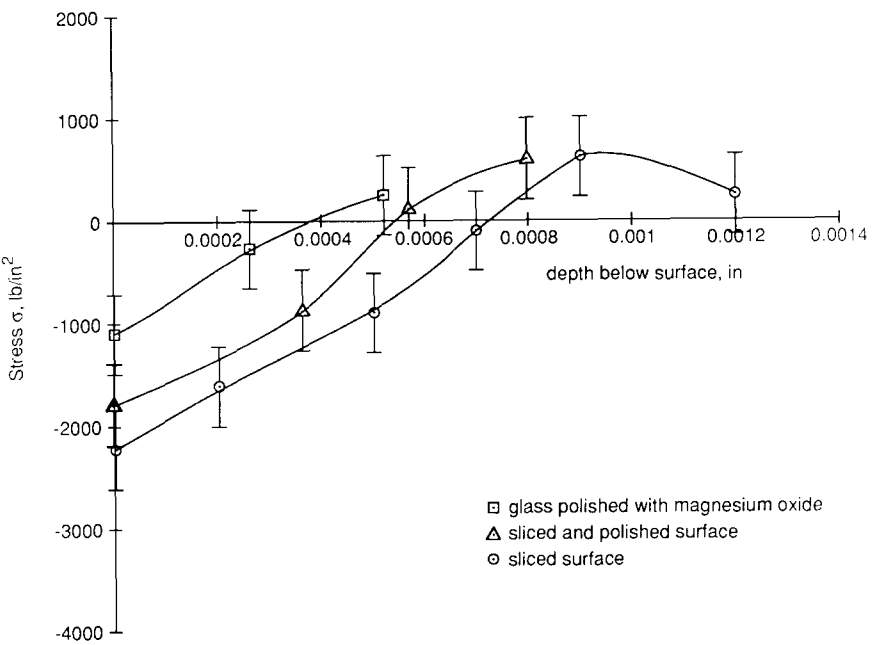

Fig. 9. Measured residual-stress distribution on flat slabs of flint glass induced by slicing and polishing processes. (Bars indicate the scatter of measurements made on five specimens.)

Fig. 8. (see opposite page). Residual stresses in typical "Rupert's drops" made of flint and silica: (a) the tensile residual stresses near the drop-axis centre-line; (b) compressive residual stresses near the surface of the drop in the direction parallel to the drop-axis centre-line; and (c) compressive residual stresses at two different locations in a flint glass-drop after annealing. (Refer to Fig. 6 for the location of the specimens used in these residual-stress measurements.) The stresses are the results of measurements on five specimens with the cross-hatched length being the scatter.

Fig. 9. The residual stresses induced by magnesium oxide polishing are biaxially compressive at ca. 1000 lb/in^2 near to the surface; this value is however of the same order as the error bars (ca. 800 lb/in^2) for the present residual-stress measurement technique under the given experimental conditions. On the glass surface that had been sliced and polished, the near-surface residual stress in Fig. 9 is again compressive at ca. 1700 lb/in^2.

Comparing the residual stresses on the quenched glass drops, see Figs. 8(a) and 8(b), with those measured on sliced and polished surfaces of glass, it can be seen that near to the axis of the drop the residual stresses are tensile, which is opposite in sign to those induced by slicing and polishing. Therefore, qualitatively at least, it is clear that tensile residual stresses exist in the glass drops near to the axis. Close to the surface of drops, the measured residual stresses are compressive, as can be seen in Fig. 8(b), but of a somewhat higher magnitude than the slicing-and-polishing residual stresses. Again it is reasonable to conclude that quenching induces compressive residual stresses near to the drop surface. For annealed drops, the measured residual stresses shown in Fig. 8(c) could possibly reflect those introduced by the preparation process.

In summary, the residual stresses along the centre-line axis of the drop are tensile in both flint glass and silica, and compressive close to the surface. Tensile stresses as high as 6000 lb/in^2 have been measured in flint glass. However, these estimates are average ones over a given area of the specimen in which stress gradients likely exist. Thus, the measured values do not accurately reflect stress magnitudes at particular locations.

7. Residual-stress calculations

Latent heat is released or absorbed during solidification and thermal stresses develop due to interaction between the temperature gradients, simultaneous hardening, and the constitutive elastic–plastic properties of the material (Levitsky and Shaffer [19]). Common examples of such stresses, both transient and residual, occur in cast and heat-treated mechanical components, in thermosetting plastics and in concrete structures such as dams.

Levitsky and Shaffer [19] analyzed the residual thermal stresses arising in a solid sphere cast from a chemically hardening material, the material properties being not unlike those of glass. Solidification was treated in their analysis as the continuous transformation of material from an inviscid liquid-like

Fig. 10. (see opposite page). Calculated residual-stress distributions in fully solidified drops: (a) radial and hoop stresses in a solid sphere cast from a chemically hardening material for several values of the Poisson's ratio (ν) of the fully hardened material (after Levitsky and Shaffer [19]). Note that the stresses and the radius shown are in arbitrary units; (b) radial and hoop stresses in a solid flint glass sphere of 6 mm diameter cooled to 25 °C in 120 s.

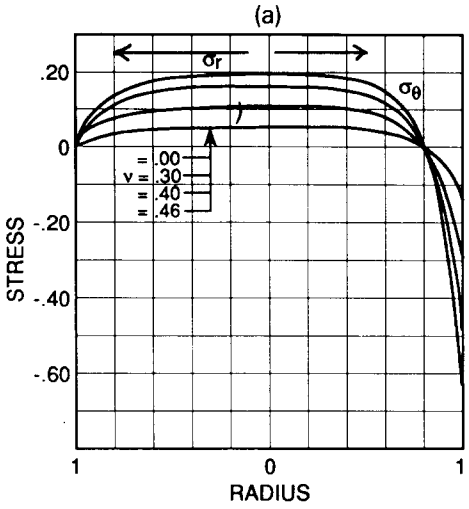
(a)
σr
σθ
.20
0
-.20
-.40
-.60
STRESS
= .00
ν = .30
= .40
= .46
1
0
1
RADIUS

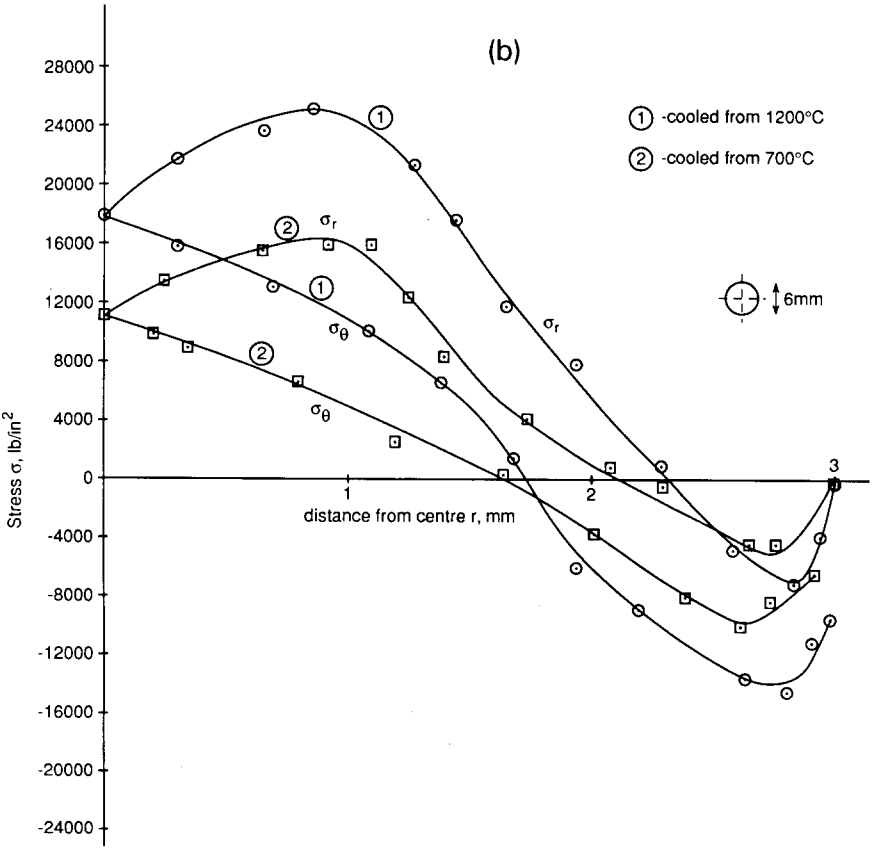
(b)
28000
24000
20000
16000
12000
8000
4000
0
-4000
-8000
-12000
-16000
-20000
-24000
Stress σ, lb/in²
① -cooled from 1200°C
② -cooled from 700°C
σr
σθ
6mm
1
2
3
distance from centre r, mm

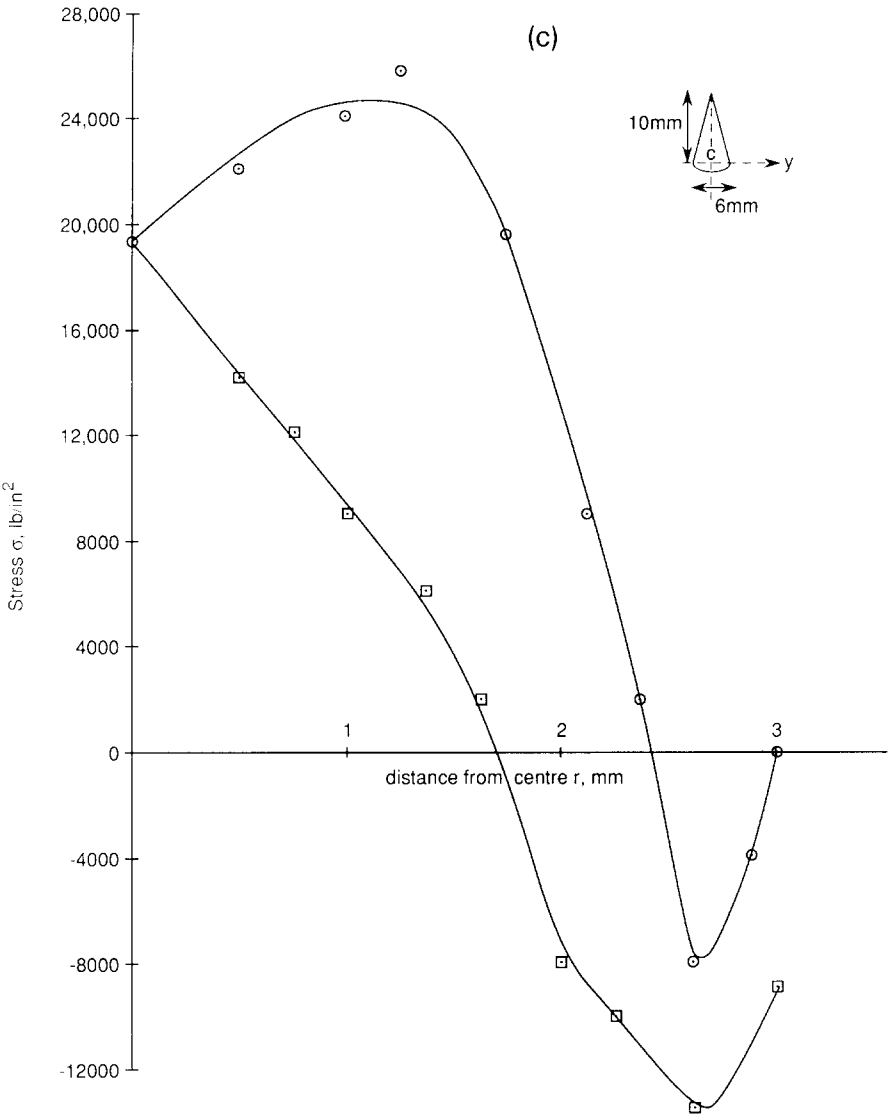

Fig. 10 (continued) (c). The radial and hoop stresses in a flint glass tear-drop cooled from 1200 °C to 25 °C in 120 s. (See inset for dimensions of the drop and the region over which the residual stresses are plotted.)

state into an elastic solid, with intermediate properties being determined by the degree of the chemical reaction.

Figure 10(a) shows the radial and circumferential residual stresses obtained by the latter authors [19] for different values of the Poisson's ratio for the fully solidified material. At the centre of the sphere the state of residual stress is one of hydrostatic tension; the circumferential stress, however, becomes

compressive near to the surface of the sphere. Their analysis showed that the magnitude of both the residual-stress components is directly proportional to the product of the bulk modulus, the coefficient of thermal expansion, and the maximum temperature rise possible during the solidification reaction. Furthermore, the compressive circumferential stress in the outer region of the sphere increases with increase in the speed of solidification.

The finite-element method was used to calculate the residual stresses developed during the solidification of a flint glass-drop when introduced into water. The calculations were carried out for two specimen geometries: (1) a sphere; and (2) a cone having a hemispherical base (tear-drop). The dimensions are given in the figure captions of Figs. 10(b) and 10(c). In both instances the glass drop was assumed to cool from an initial uniform temperature of 1200°C to a surface temperature of 25°C in 120 s, this assumption being consistent with temperature measurements on the flint glass-drop in water. The transient thermal problem was then solved to obtain the temperature distribution in the drop at different times and these distributions used as thermal loads to determine the residual-stress distribution. In the analysis, glass was modelled as a visco-elastic material. Details of the model are based on Gardon [13] and Blank [20].

A commercial finite-element package (ANSYS) was used to obtain the temperature and stress distributions. Axisymmetric quadrilateral finite elements were used. Figure 10(b) shows the calculated radial, σ_r, and hoop, σ_θ, residual stresses in a spherical glass drop of diameter 6 mm for two different cooling rates. Both the tangential and radial residual stresses are compressive near to the surface of the sphere whilst they are tensile at and near to the centre of the sphere, see Fig. 10(b). Notably, the stress state at the latter location is one of severe hydrostatic tension. The analysis also indicates, see Fig. 10(b), that, other things remaining the same, a faster rate of cooling of the sphere results in an increase in both the radial and tangential residual stresses.

Figure 10(c) shows the calculated residual stresses in a tear drop after solidification: again the radial and tangential stresses are tensile at the centre of the drop, C. These stresses are somewhat greater in magnitude than the corresponding tensile stresses at the centre of a spherical drop, the quenching conditions at the surface being the same in both cases. The greater magnitude is probably a consequence of the greater rate of cooling prevailing at the centre of the tear-drop. The near surface stresses are again compressive, see Fig. 10(c). The calculations show that the axial residual stress along the tear-drop axis (centre-line) is also tensile at the centre C of the drop; see the inset of Fig. 10(c) for its location.

The residual stresses that have been calculated are not precise regarding the magnitude of the stress state at the centre of the glass tear-drop, since the actual stress–strain behaviour of glass has been idealized as elastic–plastic in the finite element analysis, with assumed values for the variations of the yield

strength and strain hardening with temperature. In practice, glass would exhibit visco-elastic–plastic behaviour.

However, the present calculations, the earlier analytical work of Levitsky and Shaffer [19] and the present experimental measurements of the residual stresses, all demonstrate that hydrostatic tension exists along the centre-line axis of spherical and tear-shaped glass drops and compressive stresses exist under their surface, irrespective of whether the material behaves in an elastic–plastic or in a viscous-chemical-hardening manner during solidification. The hydrostatic tension near the centre of the drop could cause void nucleation and growth as observed during tear-drop solidification in a manner quite similar to the growth of voids in the "necking" region of a cylindrical specimen subject to uniaxial tension where hydrostatic tension exists. In glasses with a significantly lower coefficient of thermal expansion than flint, such as silica, the residual stresses would be expected to be much smaller in magnitude. (This was, in fact, noted in the measured residual stresses in silica.) The qualitative agreement between the residual-stress measurements and the calculations is reasonably good.

With a fairly comprehensive knowledge of the stress characteristics of the tear-drop it is worthwhile now to speculate on the reasons for the well-known disintegration or "explosion" of Rupert's drops when fractured or damaged.

8. An hypothesis for disintegration when a drop is damaged

For the purpose of analyzing the disintegration of Rupert's drops, a drop is considered as a hemisphere to the circular base of which is perfectly attached a long slender cone of small apical angle. Also kept in mind is how the analysis will be affected if there should be a paraboloid in place of the hemisphere.

Consider the two basic bodies – hemisphere and cone – separately. Now a free cone of brittle material which has a detonator exploded at the centre of its base gives rise initially to an intense compressive pulse: the head of the pulse as it travels up the axis towards the vertex develops an increasingly short, very intense head of compressive stress and a long increasingly intense tensile tail, see Fig. 11(a): this is discussed in Johnson [21]. In due course, the tensile fracture strength of the material is exceeded and a separation or fracture occurs; it is in fact likely that multiple spalling will follow, since the compressive stress ahead, trapped in the first ejected tip, generates again an increasingly great tensile stress as it proceeds further towards the apex, developing consequent fractures. Originally the situation described was quantified by Landon and Quinney [22] with respect to elastic stress waves in concrete wedges. Kolsky [23] later provided a remarkable and illuminating illustration in his book, showing the tip of a cone of Perspex "blown off" after arranging for an explosion at the centre of the base, as shown in Fig. 11(b). Subsequently All-Has-

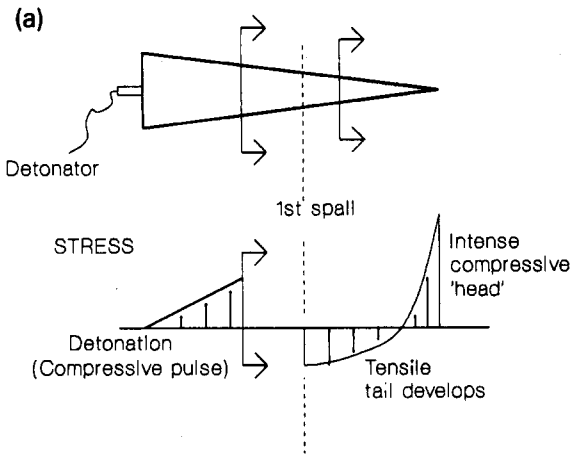

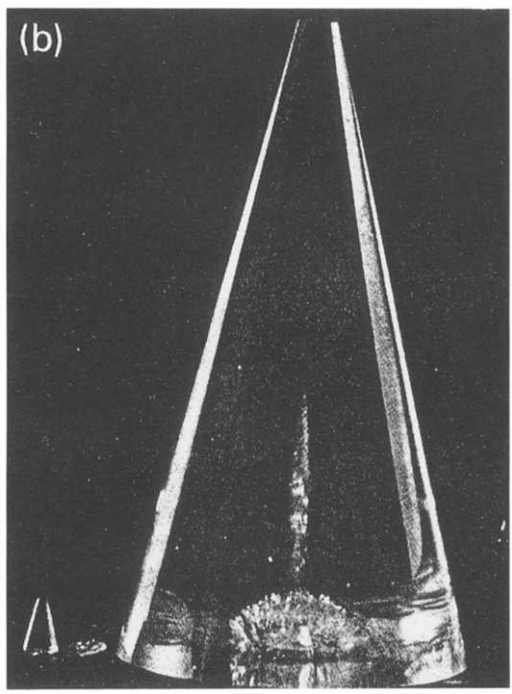

Fig. 11. Fracture due to stress waves in a cone of brittle material when a detonator is exploded at the base showing: (a) the stress state in the vicinity of the propagating wave; and (b) the fractured cone with its ejected tip (after Kolsky [23]).

sani et al. [24] did further work of this nature using triangular wedges (mostly of small angle) of brittle Plaster of Paris.

Now consider a hemisphere to which is admitted at its circular base, a compressive dilatational stress wave, P, moving parallel to the axis towards the concave hemispherical surface, see Fig. 12(a). There will be reflected from the

stress free curved surface a dilatational wave of tension P' and a shear wave S'': the tensile rays converge on one focus and the shear waves on another some small distance away. (If the incident waves had been shear waves, S, there would have been mode conversion at the stress-free boundaries to give reflected shear waves S' and dilatational waves, P''.) In all, three foci are found, see Fig. 12(b) and Lovell et al. [25]. These converging rays cause fractures on the axis of the hemisphere because of their intensifying and disruptive nature.

Putting the two bodies together as a tear-drop, it can be imagined that any artificially first-contrived fracture or damage in the conical tail of a drop, introduces an imbalance in the self-equilibrated residual stresses already present. The restoration of equilibrium proceeds by the propagation of stress waves which are both compressive and tensile (both types are initially released). Now tensile stresses propagating up the cone to the apex, will of themselves cause fracture as they intensify, whilst compressive ones will generate increasingly severe tensile tails. Compressive stress waves entering the hemispherical base will be reflected at the curved surface as tensile stress waves and be subjected to intensification as convergence or focusing occurs, over a zone approximately mid-way between the centre of the hemisphere and its surface. It is now easy to convince oneself that due to the geometry of this two-component body constituting a tear-drop, intense tensile stresses and consequently destructive

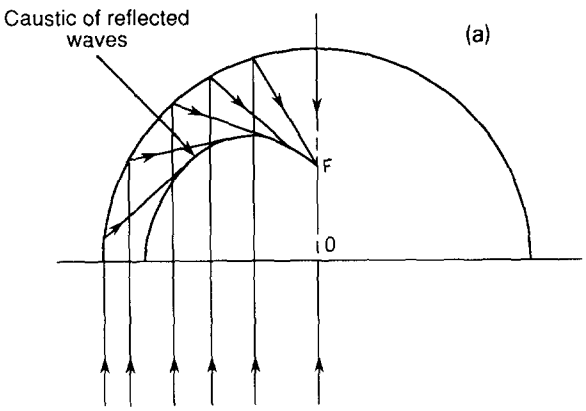

Fig. 12. Fracture due to stress waves in a hemisphere of brittle material: (a) a diagram of the reflection and convergence to the focus of a caustic curve of a compressive dilatational wave as a wave of tension.

Fig. 12 (continued; see opposite page) (b). Three high-speed photographs of the initial fracturing process in a solid sphere. Three foci are found, for each of the three different mode or wave combinations PP', PS'', SS' and SP'' (PP' and SS' have the same forms), see the text for description. Fracture or disintegration at each of the three foci is visible: (i) 49; (ii) 62.5; and (iii) 82 μs after a detonation at the South Pole.

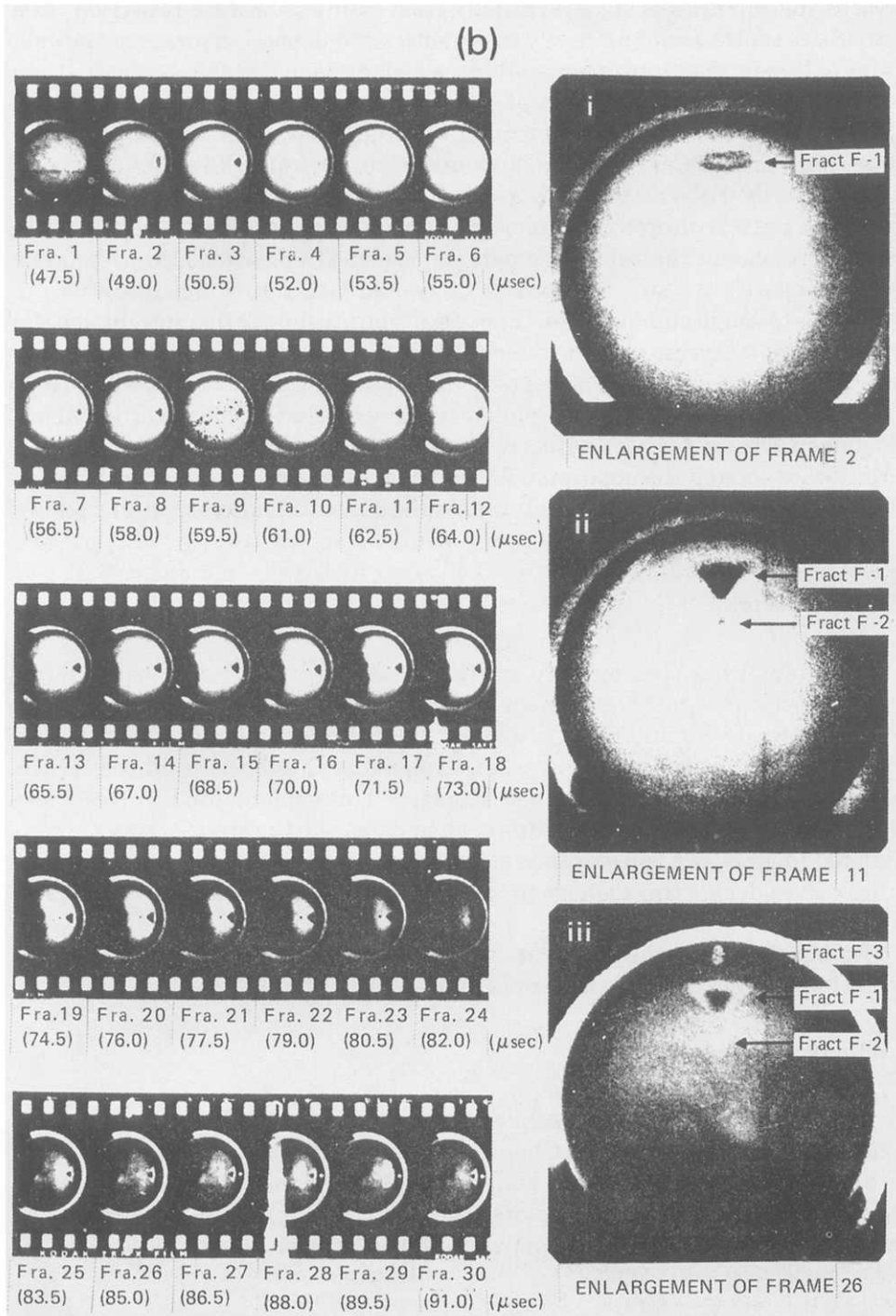
(b)
Fra. 1 (47.5)
Fra. 2 (49.0)
Fra. 3 (50.5)
Fra. 4 (52.0)
Fra. 5 (53.5)
Fra. 6 (55.0) (μsec)
Fra. 7 (56.5)
Fra. 8 (58.0)
Fra. 9 (59.5)
Fra. 10 (61.0)
Fra. 11 (62.5)
Fra. 12 (64.0) (μsec)
Fra.13 (65.5)
Fra. 14 (67.0)
Fra. 15 (68.5)
Fra. 16 (70.0)
Fra. 17 (71.5)
Fra. 18 (73.0) (μsec)
Fra.19 (74.5)
Fra. 20 (76.0)
Fra. 21 (77.5)
Fra. 22 (79.0)
Fra.23 (80.5)
Fra. 24 (82.0) (μsec)
Fra. 25 (83.5)
Fra.26 (85.0)
Fra. 27 (86.5)
Fra. 28 (88.0)
Fra. 29 (89.5)
Fra. 30 (91.0) (μsec)
i
Fract F -1
ENLARGEMENT OF FRAME 2
ii
Fract F -1
Fract F -2
ENLARGEMENT OF FRAME 11
iii
Fract F -3
Fract F -1
Fract F -2
ENLARGEMENT OF FRAME 26

fracturing will arise. They are initially created or due to wave reflections at a stress-free surface and naturally arise due to intensification processes for reasons of geometrical convergence and stress-sign changes at free surfaces. It can also be imagined that waves propagating up the cone are intersected by radial unloading waves of compression from the cone sides; intersection with compressional fracture at 45° to the forward axis of the cone should follow.

As described above, the authors have conceived of the propagating stress waves in the tear-drop as axisymmetric (and as axisymmetric in origin). However, it is evident that initiating damage, such as that introduced by bending (snapping off) towards the conical tip, would give rise to flexural waves in addition to longitudinal waves. This need not invalidate the present general view of the fracturing process; refer to the work of Miklowitz [26] who considered fracturing arising from bending. The effect of any flexural waves is to introduce additional fractures, similar to those created by the longitudinal unloading waves (associated with a decrease in the load in the fracture process). Miklowitz showed the additional fractures to arise due to interaction between the flexural waves and the longitudinal waves that are reflected from a stress-free surface.

9. Conclusions

An attempt has been made to experimentally and analytically characterize the temperatures, residual stresses and densities of Rupert's drops formed out of flint glass, Pyrex and silica. Based on this characterization and the observed fracture patterns in these glasses, an explanation has been advanced for the disintegration of these drops when damaged. This explanation involves stress wave propagation within these drops when damaged; the stress waves are considered to arise as a consequence of the internal residual stresses rearranging themselves during this damage process and attempting to reach a new equilibrated state.

An attempt to further elucidate the fracturing of small angle hemi-spherically based cones of brittle material (Perspex) is in the process of investigation.

Acknowledgements

The authors would like to acknowledge help from Mr. D. Henderson with some of the experimentation. Chandrasekar would like to acknowledge a grant from the U.S. National Science Foundation Program in Materials Engineering and Processing (Dr. R. Komanduri, Program Director) which was used in the development of the infra-red temperature measurement system.

References

1 R. Hooke, *Micrographia*, 33 (1665).
2 L. Brodsley, Sir Chas. Frank and J.W. Steeds, Prince Rupert's drops, *Notes Rec. R. Soc. London*, 41(1) (1986) 1.
3 W. Johnson, A.G. Mamalis and H. Hunt, Small spherical lead shot-forming from the liquid, using a shot tower, *Metall. Met. Form.*, March (1976) 68–73.
4 W. Johnson, Lead shot forming, Batavian drops and innovators Prince Rupert and William Watts, in: M. Kleiber and J.A. Honig (Eds.), *Inelastic Solids and Structures*, (Antoni Sawczuk Memorial Volume), Pineridge Press, Swansea, 1989, pp. 516–558.
5 Anon, *Properties of Corning's Glass and Glass Ceramic Families*, 1979.
6 N.P. Bansal and R.H. Doremus, *Handbook of Glass Properties*, Academic Press, New York, 1986.
7 W. Thomson, Notes on some of the peculiar properties of glass, *Manchester Lit. Phil. Soc.*, 2 (1889) 42.
8 S. Chandrasekar, T.N. Farris and B. Bhushan, Grinding temperatures for magnetic ceramics and steel, *ASME J. Tribology*, (1989), in press.
9 K.A. Hartley, J. Duffy and R.H. Hawley, Measurement of temperature profile during shear band formation in steels deforming at high strain rates, U.S. Army Research Office Report DAA29-85-K-003/2, 1986.
10 H.S. Carslaw and J.C. Jaeger, *Conduction of Heat in Solids*, Oxford University Press, 1947.
11 J.C. Jaeger, Conduction of heat in a solid with a power law of heat transfer at its surface, *Proc. Camb. Phil. Soc.*, 46 (1950) 634.
12 W.R. Mann and F. Wolf, Heat transfer between solids and gases under nonlinear boundary conditions, *Appl. Math.*, 9 (1951) 163.
13 R. Gardon, Thermal tempering of glass, in: D.R. Uhlmann and N.J. Kreidl (Eds.), *Glass: Science and Technology*, 5R, Academic Press, New York, 1980, p. 146.
14 D. Johnson-Walls, A.G. Evans, D.B. Marshall and M.R. James, Residual stresses in machined ceramic surfaces, *J. Am. Ceram. Soc.*, 69 (1986) 44.
15 P.W. Bridgman, *Studies in Large Plastic Flow and Fracture*, McGraw Hill, New York, 1952.
16 J.T. Hagan and M.V. Swain, The origin of median and lateral cracks around plastic indents in brittle materials, *J. Phys. D, Appl. Phys.*, 11 (1978) 2091.
17 S. Van der Zwaag and J.T. Hagan, Deformation processes in silica and different soda-lime glasses under conical indentations, in: C.R. Kurkjian (Ed.), *Strength of Inorganic Glass*, Plenum Press, New York, 1985, p. 147.
18 R.G. Treuting and W.T. Reed, A mechanical determination of biaxial residual stress in sheet materials, *J. Appl. Phys.*, 22 (1951) 130.
19 M. Levitsky and B.W. Shaffer, Residual thermal stresses in a solid sphere cast from a thermosetting material, *ASME J. Appl. Mech.*, 41(3) (1975) 651.
20 K. Blank, Some practical aspects of thermally strengthened glass, in: C.R. Kurkjian (Ed.), *Strength of Inorganic Glass*, Plenum Press, New York, 1985, p. 485.
21 W. Johnson, *Impact Strength of Materials*, Arnold, London, 1972.
22 J.W. Landon and H. Quinney, Experiments with the Hopkinson pressure bar, *Proc. R. Soc., Ser. A*, 103 (1923) 622.
23 H. Kolsky, *Stress Waves in Solids*, Dover, New York, 1963.
24 S.T.S. Al-Hassani, W. Johnson and M. Nasim, Fracture of triangular plates due to contact explosive pressure, *J. Mech. Eng. Sci., I. Mech. E*, 14 (1972) 173.
25 E. Lovell, S.T.S. Al-Hassani and W. Johnson, Fracture in solid spheres and circular disks due to a "point" explosive impulse on the surface, *Int. J. Mech. Sci.*, 16 (1974) 193.
26 J. Miklowitz, Elastic waves created during tensile fracture, *ASME J. Appl. Mech.*, 20 (1953) 122.

Appendix – Curvature technique for residual-stress measurement

A curvature technique was used to determine the residual-stress distribution on sections of the glass drops. This technique employs a very thin rectangular specimen that is polished to a high degree of flatness on one side. The residual stresses (induced by a particular process) near to the remaining parallel surface are estimated ones. The residually stressed surface is progressively etched away while the polished or reference surface is protected from being etched. After every etching step, the amount of material removed is determined by weighing as well as by measurement of the remaining thickness using a micrometer. The curvature of the reference surface is measured in the two orthogonal directions in which the principal stresses on the surface are oriented. Measurement of the curvature in a third direction also enables the directions of the principal stresses to be established.

A Talysurf profilometer is employed to determine the curvature by measuring the chordal rise over a certain length. Some of these residual-stress measurements using the latter approach have been compared with ones using X-ray diffraction and strain gauge based residual-stress estimates in various ceramics (Johnson-Walls et al. [14]). The agreement between the different residual-stress measurements was found to be good. The validity of this curvature residual-stress measurement technique has also been established in a number of earlier investigations. For more details about the curvature method and the assumptions involved, see Treuting and Reed [18] and Johnson-Walls et al. [14].

Equation (1), derived by Treuting and Reed, relates the residual stress to the measured curvatures and work-material elastic constants

$$\sigma_1(z,w_0)=\frac{E}{6(1-\nu^2)}\left[z^2\left(\frac{dC_1}{dz}+\nu\frac{dC_2}{dz}\right)+4z[C_1(z)+\nu C_2(z)]\right.$$

$$\left.+2(w_0-3z)(C_1(w_0)+\nu C_2(w_0))-2\int_z^0[C_1(z)+\nu C_2(z)]\,dz\right] \quad (1)$$

where:

$\sigma_1(z,w_0)$ and $\sigma_2(z,w_0)$ – denote the stresses in the direction in which the curvatures are measured

w_0 – initial thickness before etching

z – coordinate measuring distance below ground surface

C_1, C_2 – equilibrium curvatures of the specimen in two perpendicular directions after a layer of thickness is etched away

E – Young's modulus of the specimen

ν – Poisson's ratio of the specimen

The stresses perpendicular to the direction in question can be calculated by interchanging subscripts 1 and 2.